The structural transformation comparison of the human Prion protein mutants V176G, E196A, and I215V by using molecular dynamics simulation

Ashraf Fadhil Jomah
University of Sumer
Sepideh Parvizpour (se.parvizpour@gmail.com)
Tabriz University of Medical Sciences https://orcid.org/0000-0003-1865-5040
Jafar Razmara
University of Tabriz
Mohd Shahir Shamsir
Universiti Tun Hussein Onn Malaysia

Research Article

Keywords: Prion protein (PrP), Neurodegenerative, Molecular dynamics simulation (MD), Gerstmann-Straussler-Scheinker (GSS) syndrome

Posted Date: March 3rd, 2021

DOI: https://doi.org/10.21203/rs.3.rs-256266/v1

Abstract

The point mutations in the gene coding of prion protein (PrP) originate human familial prion protein (HuPrP) diseases. Such diseases are caused by several amino acid mutations of HuPrP including V176G, I215V, and E196A located at the second, third native helix and in their loop, respectively. Determining the transition from cellular prion protein (PrPc) to pathogenic conformer (PrPSc) in the globular domain of HuPrP that results in pathogenic mutations is the key issue. The effects of mutation on monomeric PrP are detected in the absence of an unstructured N-terminal domain only. A MD simulation for each of these wild type mutants is performed to examine their structure in the aqueous media. The structural determinants are discerned to be different for wild-type HuPrP (125–228) variants compare to that of HuPrP mutations. These three mutations exhibiting diverse effects on the dynamical properties of PrP are attributed to the variations in the secondary structure, solvent accessible surface areas (SASAs), and salt bridges in the globular domain of HuPrP. High fluctuations that are evidenced around residues of the C-terminus of the helix 1 for V176G cause Gerstmann-Straussler-Scheinker (GSS) syndrome. Conversely, the occurrence of fluctuations around residues of helix 2, helix 3, and the loss of salt bridges in these regions for E196A and I215V mutants is responsible for Creutzfeldt-Jakob disease. Furthermore, small changes in the overall SASAs mutations strongly influence the intermolecular interactions during the aggregation process. The comparative results in this study demonstrate that the three mutants undergo different pathogenic transformations.

Introduction

The neurodegenerative disease epidemic raises with the increase of life expectancy in the developed countries. It is an age-related disorder which affects both humans and animals. Prion diseases are a class of rare, fatal and progressive kind of neurodegenerative diseases including an extensive range of clinicopathological phenotypes (Lafon et al. 2018). They are distinctive infectious agents which are assembled from self-propagating multi-chain of misfolded host-encoded prion protein (PrP) (Terry and Wadsworth 2019). The human prion diseases are conventionally categorized based on their clinicopathological spectrum into Creutzfeldt–Jakob disease (as the most common), fatal insomnia, Gerstmann–Sträussler–Scheinker disease, and variably protease-sensitive prionopathy. All categories except for fatal insomnia denote heterogeneous groups comprising several distinct disease phenotypes or subtypes (Rossi et al. 2019; Zheng et al. 2018).

It is acknowledged that the major reasons for these maladies are the posttranslational transformation of the ubiquitous cellular form of the prion protein (HuPrPc) to misfolded pathogenic isoform (HuPrPSc) (Wille and Requena 2018; Wulf et al. 2017). Furthermore, without exhibiting any covalent alterations, they eventually aggregate with a defined structure (Dai et al. 2019; Vallabh et al. 2020). The quest for determining the mechanisms of Human (Hu) familial prion diseases caused by the mutations of prion protein is never-ending. The structural characteristics of PrPSc have not been entirely identified and the research is open to achieve the ultimate insight into its molecular mechanism. The main barrier in

this way is the insoluble nature of PrPSc which prevents the use of high-resolution techniques for whole determination of its structure. Thus, a partial structure of PrPSc with a low resolution is available.

It is well-known that HuPrPSc structure is rich in β-strands whereas HuPrPc mainly consists of α-helix in secondary structure conformation. The structures obtained from NMR reveal a C-terminal globular domain from residue 125 to 228 (human numbering) and an N-terminal flexible disordered tail (Poggiolini et al. 2013). The globular domain is composed of three α-helices forming the residues 144–154 helix 1, 173–194 helix 2, and 200–228 helix 3 as well as a very short anti-parallel β-sheet with residues 128–131 b1 and 161–164 b2. Also, a disulphide bond (Cys179–Cys214) connects helices 2 and 3. Regions of helix 2 and 3 play a decisive role in transforming HuPrPc to HuPrPSc (Castle and Gill 2017; Zheng et al. 2018).

The studies revealed that 40 mutation points in the PrP gene coding originate human familial prion diseases. These mutations mostly happen in the protein globular domain (Guo et al. 2012a; Rossetti et al. 2011). The disease mediated by these mutations causes the spontaneous generation of HuPrPSc in the brain. The misfolding kinetics of HuPrP wild type (WT) as well as the stability of partially folded intermediate species such as HuPrPSc precursors are enhanced by the presence of thermodynamic instability in PrPc (Rossetti et al. 2011). Further investigation of the mutated structure of the PrP molecules reveals the role of their misfolding in different types of spontaneous illness in human even without the existence of infection from exogenous sources (Biasini et al. 2008; Jeffrey et al. 2009). Consequently, the instability in PrP mutants also amplifies the likelihood of misfolding which may be ignored from the quality control cellular pathway and multiplied within cell (Doss et al. 2013).

In this study, four prion systems including three pathogenic mutant diseases caused by the mutation of V176G (Ashraf Fadhil Jomah 2016) and E196A (Wu et al. 2020) and I215V (Munoz-Nieto et al. 2013) at codon 129 and a WT (HuPrP) were simulated using MD of 100 ns. The mechanisms causing human familial prion diseases such as CJD and GSS were established. These PrP systems also were investigated for their physicochemical properties such as hydrophobicity, solvent accessibility, and salt bridge. Results on the structural disorder of mutation clusters in the globular HuPrP domain revealed useful insight.

Materials And Methods

Study design

Four prion systems consisting of WT HuPrP (125-228) and three pathogenic mutants such as HuPrP (V176G), HuPrP (E196A), and HuPrP (I215V) are considered for the 100 ns MD simulation (Muñoz-Nieto et al. 2013; Simpson et al. 2013; Zhang et al. 2014). The relevant protein files and 3D model structures are extracted from the standard Protein Data Bank (PDB). NMR structure coordinates of HuPrP are used to simulate WT at pH 7 (PDB code:1QLX) where the residue numbers are altered from 125–228 to 0–103. The diseases caused by such HuPrP mutant structures are achieved by incorporating the mutation

on the NMR WT HuPrP via Pymol. Figure 1 shows the methionine and valine polymorphisms that are preserved for these mutants at codon-129.

Molecular Dynamics Simulation

The GROMACS 5.0.7 software package and all-hydrogen function GROMOS96 were employed to run MD simulations over 100 ns (Parvizpour et al. 2019). The simulations were done in the aqueous solution using a water molecule cubic box with a vector size of 7.08 nm for all prion systems. The protonation states of the ionizable residues are adjusted to maintain the neutral pH conditions regarding their pKas, using Na ions as counter ions. Periodic boundary conditions in the NPT ensemble are used at a fixed pressure (P = 1 bar) and temperature (T= 300 K). The Ewald particle mesh (PME) is used to treat long-range electrostatic interactions.

Structural Analyses

All of the resulting trajectories are analyzed using GROMACS utilities and results are recorded for a representative trajectory. The Cα root mean square deviations (RMSD) and its fluctuations (RMSF) relative to the average MD structure, solvent accessible surface areas (SASAs), and salt bridges (SBs) are computed (Mohammadi et al. 2018; Parvizpour et al. 2017). The percentage of secondary structure throughout the simulations is determined using the DSSP program. Images of protein structure are generated using Pymol and VMD tools.

Results

RMSDs of C_α Atom

The C_α RMSDs as shown in Figure 2 is acquired from the backbone of four model structures of the globular domain (residues 128–225) after 50000 ps. Weak fluctuations in the range of 0.2-0.3 nm are observed for most of the simulations. Furthermore, a slight increase in RMSD fluctuation in the range of 0.4-0.45 is observed for I215V as shown in Figure 2C. RMSD for all three mutant molecules follow the different degrees of variations and overlap with WT at 1.5 ns. The variations associated with V176G and I215V staggered the entire simulations as displayed in Figure 2A, 2C. The fluctuations of WT and E196A are twisted together from 3 to 100 ns as illustrated in Figure 2B. A relatively higher average RMSD response (100 ns) for I215V mutant than wild-type mutant structures is observed. This is ascribed to the higher structural instability of I215V compare to WT PrP structure. This higher response arises from the strong conformational change in their molecular structure. RMSD value for WT structure is found to be higher than that of the V176G mutant as depicted in Figure 2A. Thus, these deviations in the mutant structure caused by the disease display unusual features (Simpson et al. 2013).

RMSFs of C_α Atom

The RMSFs display significant initial fluctuations. Irrespective of runs, the structures exhibit random fluctuations in the residues range of 3-29. All mutants consist of a loop, β-strand, and helix 1 structures. The minimum fluctuations are evidenced for helix 2 and helix 3 regions associated with a single disulphide bridge. Conversely, the maximum fluctuations are appeared in the helix 1 region (residues 19–29) for V176G and other mutants. However, the RMSF values as shown in Figure 3A are observed to be very stable for V176G in helix 2 (residues 48–69) and helix 3 (residues 75-103). Mutants E196A and I215V corresponding to helix 2 and helix 3 regions are detected to be more flexible (less stable) than WT as illustrated in Figures 3B and 3C. In all cases the higher RMSFs for HuPrP mutants compare to that of WT PrP indicates their lower rigidity. Furthermore, the amino acid substitutions at helix 2, helix 3, and within their loop introduce more flexibility due to long range interactions. Truly, these interactions are responsible for the fluctuations in mutant structures and influence the stability of PrP. Mutations might have some local impact on the protein interactions which are required for oligomerization into fibrillar species (Behmard et al. 2011).

Percentage of Secondary Structure

The secondary structural elements of HuPrP mutants and WT as displayed in Figure 4 are appeared to be largely preserved in all mutated systems over 100 ns timescale. In comparison to WT Figure 4A, the structural contents of helix 2 in V176G Figure 4B show a shift from helix to turn the structures in helix 3. Conversely, helix 2 of E196A Figure 4C and helix 3 of I215V Figure 4D reveals weak growth without any significant increase in β-sheet. Consequently, based on the structural perspective it is difficult to realize the conformational transitions of PrPc to PrPSc resulted from mutations.

Salt Bridges (SBs)

Salt bridges play a decisive role to stabilize both secondary and tertiary structures of PrPc. Even a small disruption of SBs causes substantial destabilization of the folded conformation which possibly accelerates or enables the transition of PrPc into PrPSc. Mutations can disrupt the native SB networks (Rossetti et al. 2011). Seven SBs including E211_R208, E207_K204, E207_R208, E200_K204, E196_R156, E146_K204, and D202_R156 which involve helix 1, 2, and 3 of WT and HuPrP mutants are considered here. They connect the region of helix 2 with 3 and the C-terminal of helix 1 and 3. The regions of helix 2 and 3 lose the SBs network completely or partially within itself and with helix 1. The appearance of abolished SBs is due to HuPrP mutants V176G and E196A. The SBs resulted from the mutations within helix 2 are found to be weak. This observation is inconsistent with the earlier reports (Guo et al. 2012b; Rossetti et al. 2011). The complete or partial loss of SBs in mutated PrP leads to its destabilization in helix 1 for V176G, in helix 2 for E196A, and helix 3 for I215V.

Hydrophobicity and Solvent Accessible Surface Area (SASA)

The most important features of protein misfolding and aggregation are described by hydrophobicity and SASA parameters. Estimations of these quantities are essential to determine the stability of secondary and tertiary structural elements of PrPs (van der Kamp and Daggett 2010). (Table 1) displays the

computed values of hydrophobicity and SASA for HuPrP mutants. The hydrophobicity for each mutant V176G, E196A, and I215V reveals an increase compared to WT. However, the value of SASA for both E196A and I215V is increased and for V176G is decreased in comparison to WT. The electrostatic potential surfaces of all mutants are depicted in Figure 6. All mutated regions exhibit more color changes compared to that of WT. The electrostatic potential redistributions may influence the intermolecular recognition and interactions between PrPSc and PrPc or the aggregation of PrPSc (Guo et al. 2012b).

Discussion

Single-amino-acid substitutions such as M/V129 isoforms and pathogenic mutations identified in inherited prion diseases can influence a person's susceptibility to develop the syndrome. Structural studies with HuPrP variants containing familial mutations provide important clues regarding the molecular basis of the disease. MD simulations provide a better understanding regarding the interactions such as hydrogen bonding, hydrophobic, and electrostatic as a function of environment and motion in a variety of biological systems (Gong et al. 2010). Recently, many MD studies including G131V, S132I, A133V, D178N, V180I, T183A, H187R, F198S, E200K, V203I, V210I, and Q212P mutations are performed (Behmard et al. 2011; Guo et al. 2012b; Shamsir and Dalby 2005). It is established that the major role of inherited point mutations is to enhance the likelihood of misfolding by the thermodynamic destabilization of PrPc. This in turn triggers an abnormal interaction with other cofactors or promotes an aberrant accumulation inside the cell. Based on the experimental evidence it is postulated that the effect of inherited point mutations on the HuPrP structure results in the spontaneous formation of PrPSc in the brain. One of the key issues is the identification of the regions involved in the transition process from α-helical to β-sheet rich structure. Several studies propose that the region between helix 2 and 3 plays a crucial role during the conversion of PrPc into PrPSc (Adrover et al. 2010).

Our MD simulation results on the dynamical behavior of the globular domain of WT and the HuPrP mutants (V176G, E196A, and I215V) reaffirm the earlier observations. It is demonstrated that different amino acid substitutions produce some subtle effects on the structural features of PrP. Although, helix 1 reveals higher fluctuations compare to WT for V176G but both helix 2 and 3 remain very stable. However, mutants E196A and I215V show the opposite behavior compare to V176G. The fluctuations grow up in helix 2 and 3 but remain more stable in helix 1. The contents of β-sheet do not increase in mutated PrPSc as expected. The disruption of a specific SB network present in WT and mutants in all disease linked mutations consequently increase the flexibility of helix 1 for V176G and helix 2 and 3 for E196A and I215V. The residues involved in the SBs are highly conserved and their absence is ascribed to the pathogenic behaviors (Adrover et al. 2010). The formation of PrPSc is assigned to the disruption of native SBs and transfer of some charged groups in a low permittivity environment.

It is further observed that the alterations in the charge state of a mutant protein tend to form aggregates and the aggregation propensity of a polypeptide chain is inversely correlated with its net charge. Thus, point mutations strongly affect the kinetics of amyloid formation. The core of PrPSc amyloid is observed to be in favor of a low dielectric and hydrophobic environment (Adrover et al.

2010; Guest et al. 2010). Much of these destabilizing mutations are found to be located in the central hydrophobic core of PrP (Guo et al. 2012b). A region can be defined as interacting residues with purely hydrophobic side chains that form the core of the globular domain. We assert that the hydrophobic core is important for the stability of the globular domain of PrP.

Conclusion

The change in human prion protein in residues located within sequences of HuPrP caused by mutation is simulated. Structural variations in WT PrP and disease related mutations caused by V176G and E196A (carrying valine) and I215V (carrying Methionin) at codon 129 are compared to determine the impacts of mutation on monomeric PrP. The MD simulation of 100 ns performed for wild type and each of these mutants in the globular domain is found to be fairly conserved between WT and mutants. The changes in the secondary structures and local fluctuations are very small upon mutations. Three mutations are found to have diverse effects on the dynamical properties of PrP causing variations in the secondary structure, SASAs, and salt bridges in the globular domain of HuPrP. Furthermore, high fluctuations occur around residues of the C-terminus of the helix 1 for V176G compare to other mutants such as E196A and I215V display somewhat unusual constellation of molecular dynamic features. Our analyses reveal the conformational fluctuations in the mutant's structure. The mechanism of the transformation of PrPc to PrPSc that results in prion diseases is established. The domain in the C-terminal end of the protein plays a significant role in transforming PrPc to PrPSc and results in most of the pathogenic mutations within this part of the protein is focused without considering unstructured N-terminal.

Declarations

Acknowledgments

The authors are grateful to thank Mr. T.H. Chew for his kind technical assistance at Universiti Teknologi Malaysia.

Declarations

Funding

None.

Competing interests

The authors declare no conflicts of interest.

Availability of data and material

None.

Code availability

None.

Authors' contribution

AFJ and SP: designing and running the simulations; MSS: supervision; AFJ, SP, JR, MSS: writing and reviewing the manuscript.

Ethics approval

The authors declare no ethical issue to be considered.

Consent to participate

Not applicable to this article, since data of this study do not involve human participants.

Consent for publication

Not applicable to this article, since data of this study do not involve human participants.

References

1. Adrover M, Pauwels K, Prigent S, de Chiara C, Xu Z, Chapuis C, Pastore A, Rezaei H (2010) Prion fibrillization is mediated by a native structural element that comprises helices H2 and H3. J Biol Chem 285(27):21004–21012
2. MOLECULAR DYNAMIC SIMULATION OF V176G MUTATION ASSOCIATED WITH GERSTMANN–STRÄUSSLER–SCHEINKER AT ELEVATED TEMPERATURE (2016) Jurnal Teknologi 78(2):99–105. doi:10.11113/JT.V78.5200
3. Behmard E, Abdolmaleki P, Asadabadi EB, Jahandideh S (2011) Prevalent mutations of human prion protein: A molecular modeling and molecular dynamics study. Journal of Biomolecular Structure Dynamics 29(2):379–389
4. Biasini E, Medrano AZ, Thellung S, Chiesa R, Harris DA (2008) Multiple biochemical similarities between infectious and non-infectious aggregates of a prion protein carrying an octapeptide insertion. Journal of neurochemistry 104(5):1293–1308
5. Castle AR, Gill AC (2017) Physiological Functions of the Cellular Prion Protein. Front Mol Biosci 4:19. doi:10.3389/fmolb.2017.00019
6. Dai Y, Lang Y, Ding M, Zhang B, Han X, Duan G, Cui L (2019) Rare genetic Creutzfeldt-Jakob disease with E196A mutation: a case report. Prion 13(1):132–136. doi:10.1080/19336896.2019.1631679
7. Doss CGP, Rajith B, Rajasekaran R, Srajan J, Nagasundaram N, Debajyoti C (2013) In Silico Analysis of Prion Protein Mutants: A Comparative Study by Molecular Dynamics Approach. Cell Biochem Biophys 67(3):1307–1318

8. Gong Z, Zhao Y, Xiao Y (2010) RNA stability under different combinations of amber force fields and solvation models. Journal of Biomolecular Structure Dynamics 28(3):431–441
9. Guest WC, Cashman NR, Plotkin SS (2010) Electrostatics in the stability and misfolding of the prion protein: salt bridges, self energy, and solvation This paper is one of a selection of papers published in this special issue entitled “Canadian Society of Biochemistry, Molecular & Cellular Biology 52nd Annual Meeting-Protein Folding: Principles and Diseases” and has undergone the Journal's usual peer review process. Biochemistry and Cell Biology 88(2):371–381
10. Guo J, Ning L, Ren H, Liu H, Yao X (2012a) Influence of the pathogenic mutations T188K/R/A on the structural stability and misfolding of human prion protein: Insight from molecular dynamics simulations. Biochimica et Biophysica Acta (BBA)-General Subjects 1820(2):116–123
11. Guo J, Ren H, Ning L, Liu H, Yao X (2012b) Exploring structural and thermodynamic stabilities of human prion protein pathogenic mutants D202N, E211Q and Q217R. J Struct Biol 178(3):225–232
12. Jeffrey M, Goodsir C, McGovern G, Barmada SJ, Medrano AZ, Harris DA (2009) Prion protein with an insertional mutation accumulates on axonal and dendritic plasmalemma and is associated with distinctive ultrastructural changes. Am J Pathol 175(3):1208–1217
13. Lafon PA, Imberdis T, Wang Y, Torrent J, Robitzer M, Huetter E, Alvarez-Martinez MT, Chevallier N, Givalois L, Desrumaux C, Liu J, Perrier V (2018) Low doses of bioherbicide favour prion aggregation and propagation in vivo. Scientific reports 8(1):8023. doi:10.1038/s41598-018-25966-9
14. Mohammadi S, Parvizpour S, Razmara J, Abu Bakar FD, Illias RM, Mahadi NM, Murad AM (2018) Structure Prediction of a Novel Exo-beta-1,3-Glucanase: Insights into the Cold Adaptation of Psychrophilic Yeast Glaciozyma antarctica PI12. Interdisciplinary sciences. computational life sciences 10(1):157–168. doi:10.1007/s12539-016-0180-9
15. Munoz-Nieto M, Ramonet N, Lopez-Gaston JI, Cuadrado-Corrales N, Calero O, Diaz-Hurtado M, Ipiens JR, Ramon y Cajal S, de Pedro-Cuesta J, Calero M (2013) A novel mutation I215V in the PRNP gene associated with Creutzfeldt-Jakob and Alzheimer's diseases in three patients with divergent clinical phenotypes. J Neurol 260(1):77–84. doi:10.1007/s00415-012-6588-1
16. Muñoz-Nieto M, Ramonet N, López-Gastón JI, Cuadrado-Corrales N, Calero O, Díaz-Hurtado M, Ipiens JR, y Cajal SR, de Pedro-Cuesta J, Calero M (2013) A novel mutation I215V in the PRNP gene associated with Creutzfeldt–Jakob and Alzheimer’s diseases in three patients with divergent clinical phenotypes. Journal of neurology 260(1):77–84
17. Parvizpour S, Razmara J, Pourseif MM, Omidi Y (2019) In silico design of a triple-negative breast cancer vaccine by targeting cancer testis antigens. Bioimpacts 9(1):45–56. doi:10.15171/bi.2019.06
18. Parvizpour S, Razmara J, Shamsir MS, Illias RM, Abdul Murad AM (2017) The role of alternative salt bridges in cold adaptation of a novel psychrophilic laminarinase. Journal of Biomolecular Structure Dynamics 35(8):1685–1692
19. Poggiolini I, Saverioni D, Parchi P (2013) Prion protein misfolding, strains, and neurotoxicity: an update from studies on Mammalian prions. Int J Cell Biol 2013:910314 doi:10.1155/2013/910314

20. Rossetti G, Cong X, Caliandro R, Legname G, Carloni P (2011) Common structural traits across pathogenic mutants of the human prion protein and their implications for familial prion diseases. Journal of molecular biology 411(3):700–712
21. Rossi M, Baiardi S, Parchi P (2019) Understanding Prion Strains: Evidence from Studies of the Disease Forms Affecting Humans. Viruses 11(4) doi:10.3390/v11040309
22. Shamsir MS, Dalby AR (2005) One gene, two diseases and three conformations: molecular dynamics simulations of mutants of human prion protein at room temperature and elevated temperatures. Proteins: Structure, Function, and Bioinformatics 59(2):275–290
23. Simpson M, Johanssen V, Boyd A, Klug G, Masters CL, Li Q-X, Pamphlett R, McLean C, Lewis V, Collins SJ (2013) Unusual Clinical and Molecular-Pathological Profile of Gerstmann-Sträussler-Scheinker Disease Associated With a Novel PRNP Mutation (V176G). JAMA neurology 70(9):1180–1185
24. Terry C, Wadsworth JDF (2019) Recent Advances in Understanding Mammalian Prion Structure: A Mini Review. Front Mol Neurosci 12:169. doi:10.3389/fnmol.2019.00169
25. Vallabh SM, Minikel EV, Schreiber SL, Lander ES (2020) Towards a treatment for genetic prion disease: trials and biomarkers. Lancet Neurol 19(4):361–368. doi:10.1016/S1474-4422(19)30403-X
26. van der Kamp MW, Daggett V (2010) Pathogenic mutations in the hydrophobic core of the human prion protein can promote structural instability and misfolding. Journal of molecular biology 404(4):732–748
27. Wille H, Requena JR (2018) The Structure of PrP(Sc) Prions. Pathogens 7(1) doi:10.3390/pathogens7010020
28. Wu X, Cui Z, Guomin X, Wang H, Zhang X, Li Z, Sun Q, Qi F (2020) Rare genetic E196A mutation in a patient with Creutzfeldt-Jakob disease: a case report and literature. Prion 14(1):143–148. doi:10.1080/19336896.2020.1769528
29. Wulf MA, Senatore A, Aguzzi A (2017) The biological function of the cellular prion protein: an update. BMC Biol 15(1):34. doi:10.1186/s12915-017-0375-5
30. Zhang H, Wang M, Wu L, Zhang H, Jin T, Wu J, Sun L (2014) Novel prion protein gene mutation at codon 196 (E196A) in a septuagenarian with Creutzfeldt–Jakob disease. Journal of Clinical Neuroscience 21(1):175–178
31. Zheng Z, Zhang M, Wang Y, Ma R, Guo C, Feng L, Wu J, Yao H, Lin D (2018) Structural basis for the complete resistance of the human prion protein mutant G127V to prion disease. Scientific reports 8(1):13211. doi:10.1038/s41598-018-31394-6

Table

Table 1. The average value of hydrophobicity and total SASA for all mutants.

Properties $(nm)^2$	WT	V176G	E196A	I215V
Hydrphobicity	33.11	33.82	33.52	33.72
SASA	72.12	71.27	72.32	74.05

Figures

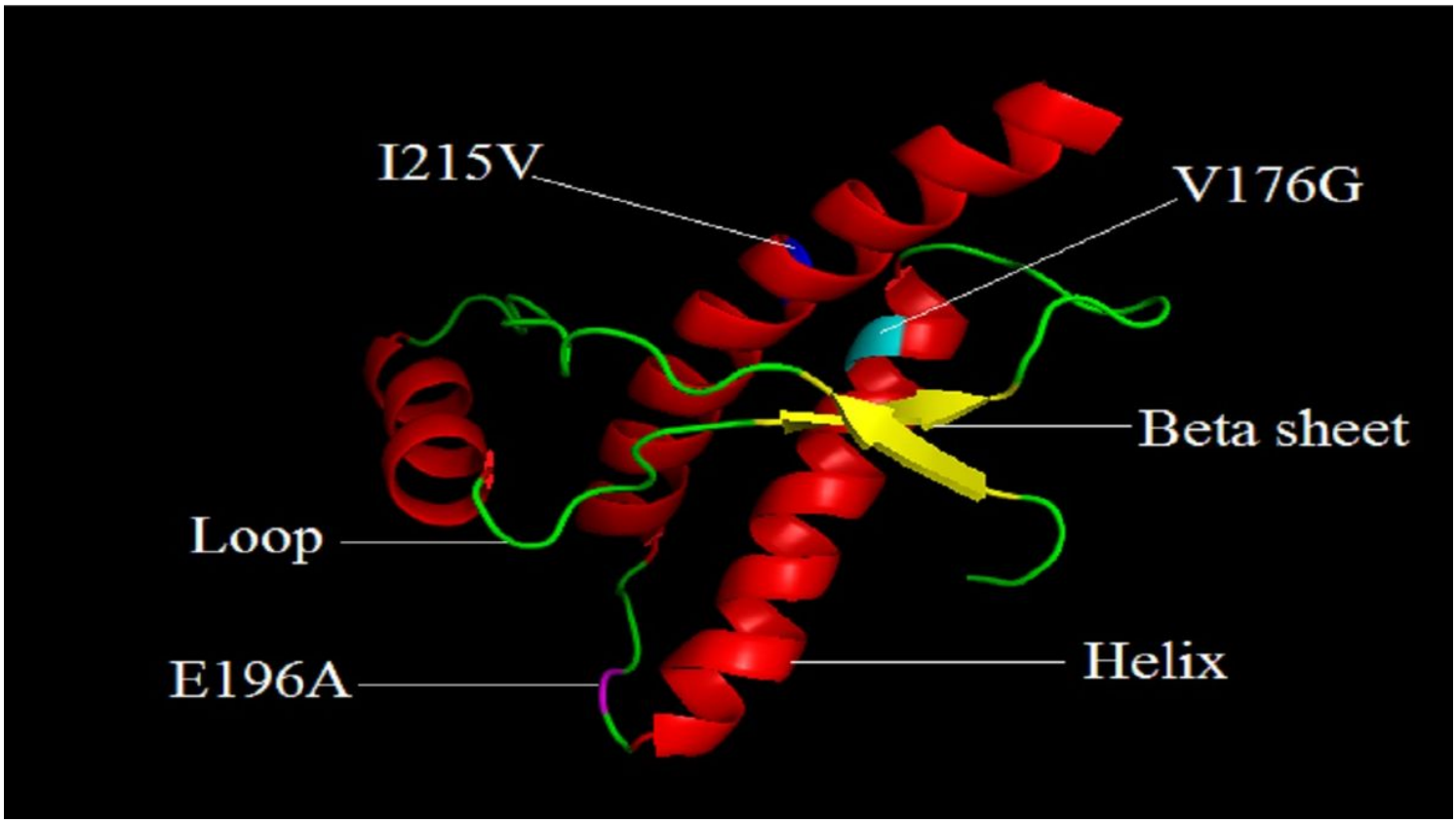

Figure 1

Structure of globular domain of WT HuPrP (PDB ID: 1QLX), residues 125–228, and the mutated residues displayed as sticks via Pymol.

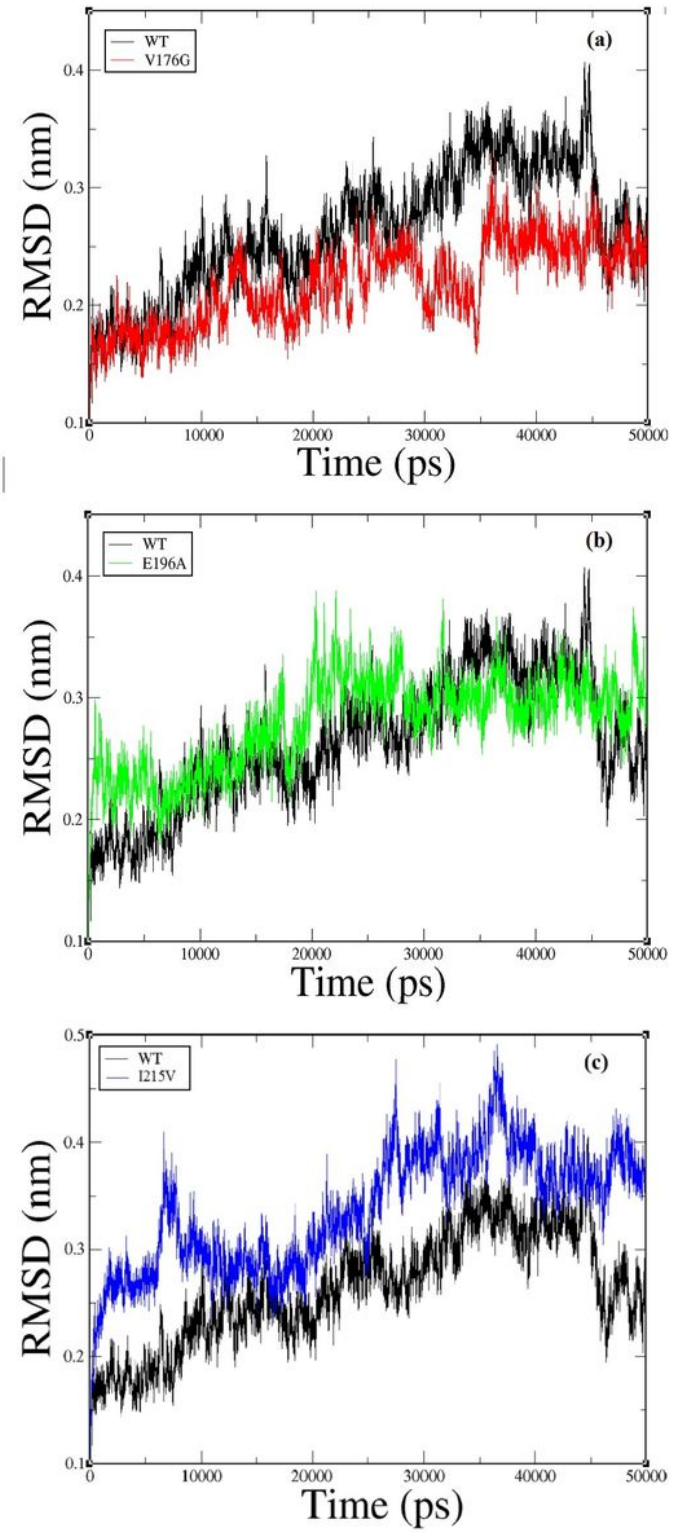

Figure 2

Cα RMSD obtained from the structure of the globular domain (residues 128–225) for HuPrP mutants (a) V176G, (b) E196A, and (c) I215V.

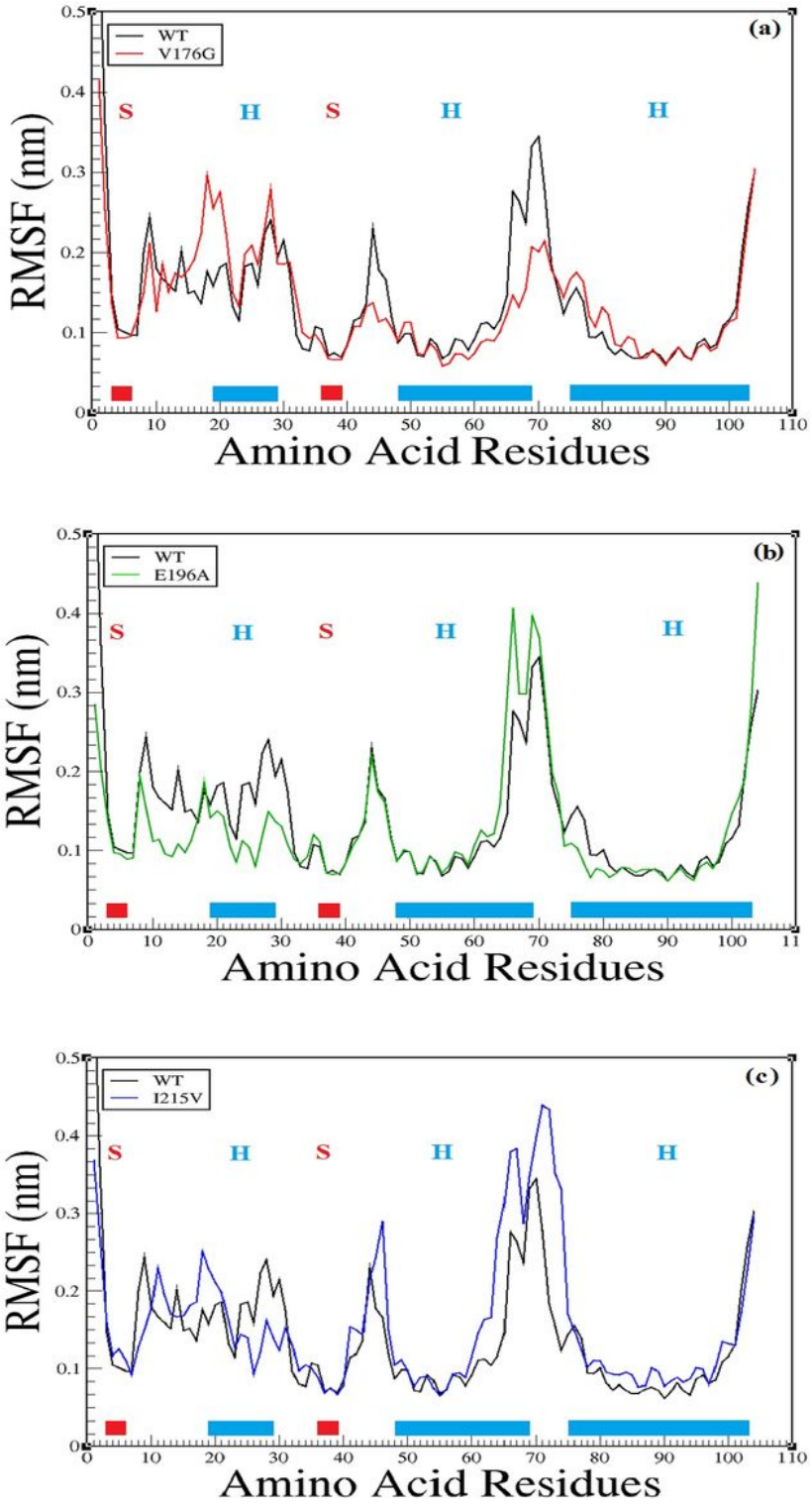

Figure 3

Cα RMSF obtained from the structure of the globular domain (residues 0–103) for mutants (a) V176G, (b) E196A, and (c) I215V. S and H stand for sheets and helices.

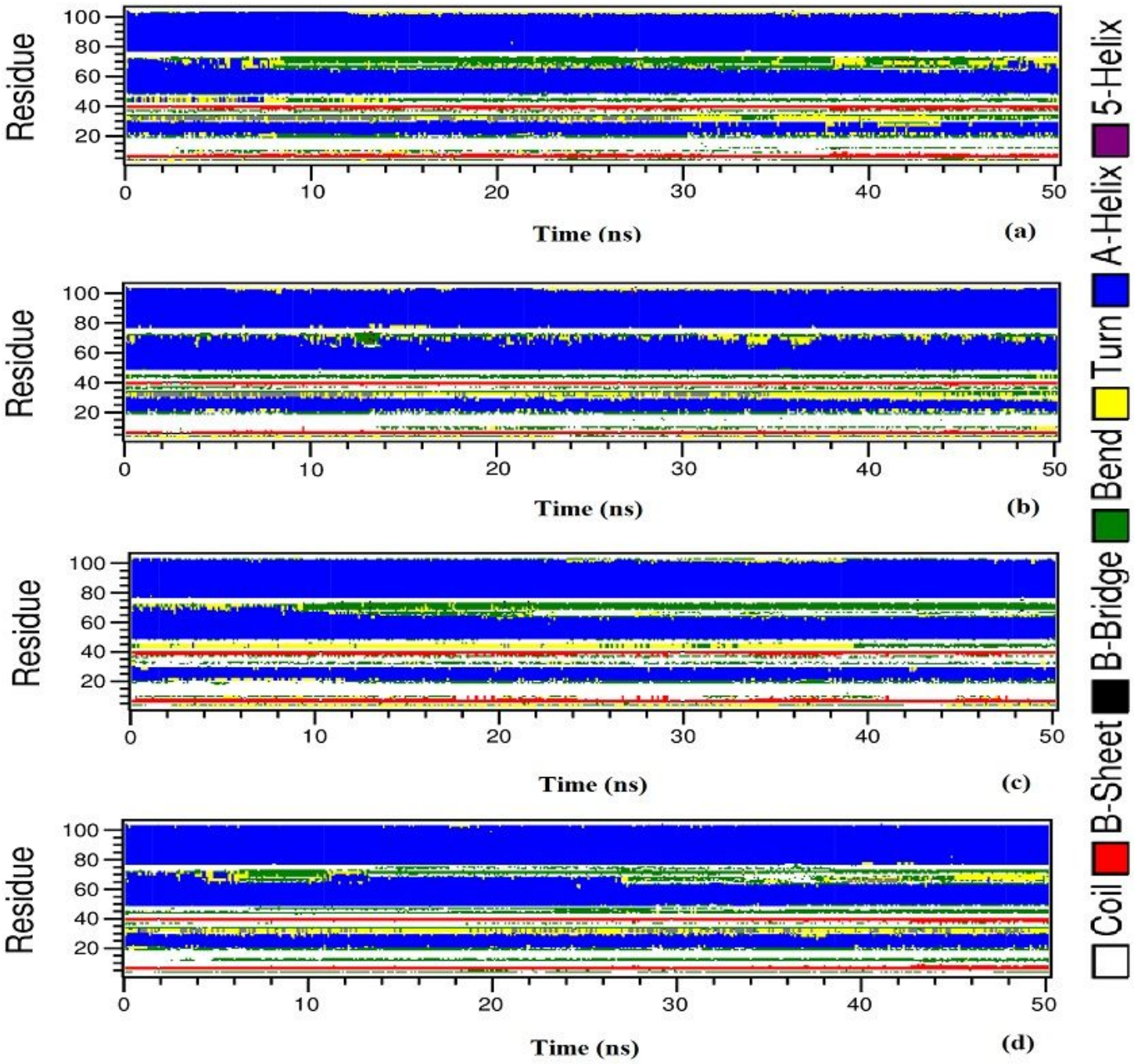

Figure 4

Secondary structure analysis based on the DSSP algorithm for (a) WT, (b) PrP mutant V176G, (c) PrP mutant E196A, and (d) PrP mutant I215V.

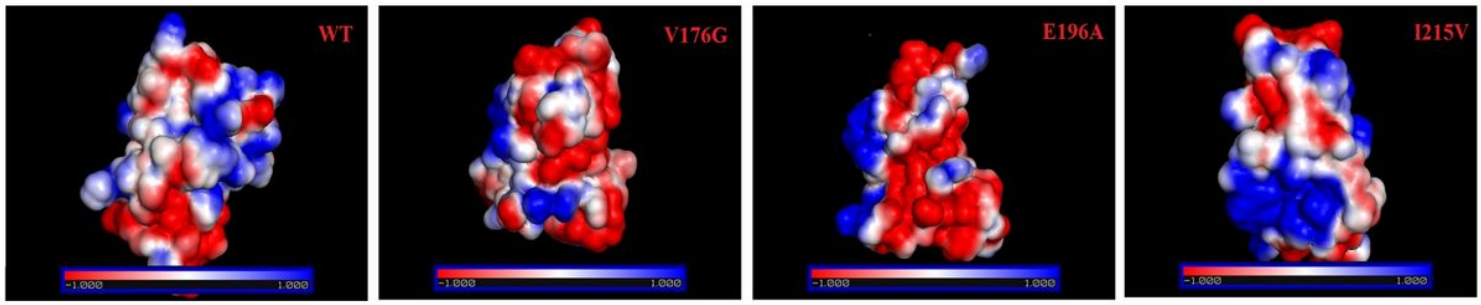

Figure 5

The electrostatic potential surface of all mutants was obtained via Pymol. The blue and red colors correspond to positive and negative electrostatic potentials, respectively).